Microscopic patterning of orientated mesoscopic silica through guided growth

M. Trau*†‡‖, N. Yao†‖, E. Kim§, Y. Xia§, G. M. Whitesides§ & I. A. Aksay*†

** Department of Chemical Engineering and †Princeton Materials Institute, Princeton University, Princeton, New Jersey 08544-5263, USA*
§ Department of Chemistry, Harvard University, Cambridge, Massachusetts 02138-2902, USA
‖ These authors contributed equally to this work

The supramolecular assembly of surfactant molecules at a solid–liquid interface can produce tubular structures with diameters of around 10 nm (refs 1–4), which can be used for the templated polymerization of mesoporous silica thin films[3–5]. The orientation of the tubules depends primarily on the nature of the substrate–surfactant interaction. These nanostructured films hold much promise for applications such as their use as orientated nanowires[6], sensor/actuator arrays[7–9] and optoelectronic devices[10]. But a method of patterning the tubules and orientating them into designed arrangements is required for many of these possibilities to be realized. Here we describe a method that allows the direction of growth of these tubules to be guided by infiltrating a reaction fluid into the microcapillaries of a mould in contact with a substrate[11]. An electric field applied tangentially to the surface within the capillaries induces electro-osmotic flow, and also enhances the rates of silica polymerization around the tubules by localized Joule heating. After removal of the mould, patterned bundles of orientated nanotubules remain on the surface. This method permits the formation of orientated mesoporous channels on a non-conducting substrate with an arbitrary microscopic pattern.

The development of low-cost lithographic techniques to pattern materials with structural features on the nanometre scale is important for the miniaturization of electronic, optoelectronic and magnetic devices. Existing approaches include technologies involving scanning electron beams[12,13], X-ray lithography[14,15], scanning probe microscopes[16,17] and imprinting methods[18]. The 'micromoulding in capillaries' (MIMIC) technique[11] provides a low-cost approach to thin-film patterning. In this method, a network of patterned capillaries is formed by placing an elastomeric stamp (typically made of polydimethyl siloxane, PDMS) possessing designed relief features on its surface in contact with a flat substrate (see Fig. 1). Second, an acidified aqueous reacting solution of tetraethoxysilane (TEOS) and cetyltrimethylammonium chloride (CTAC) is placed in contact with the edge of the mould and is transferred by 'wicking' into the networked channels. Typical molar ratios for the reacting solution are 1 TEOS : 1.2 CTAC : 9.2 HCl : 1,000 H_2O. As has been shown previously[4], the formation of a mesoscopic silica film begins to occur immediately on contact of this solution with any interface onto which the surfactant can adsorb. A dilute solution of the TEOS silica source is specifically used to prevent homogeneous nucleation of inorganic material in bulk solution, and to promote heterogeneous nucleation and growth of a mesoscopic film at the substrate–solution interface[4].

Within the capillaries, because the reacting solution is dilute, reactants are quickly depleted, and film growth ceases if wicking occurs only through capillary suction. Moreover, the growth of mesoscopic film at the edges of the mould seals the capillaries and prevents diffusion of reacting species to the interior of the mould. Therefore, to maintain a uniform concentration of reactants within the capillaries during the growth process, we applied an electric field parallel to the substrate in the manner shown in Fig. 1. Application of an electric field in this geometry has three effects: it induces electro-osmotic fluid flow; it aligns surfactant tubules; and it causes localized Joule heating of the solution. These effects are synergistic in guiding and polymerizing the silicate mesostructures within the microcapillary reaction chambers. For applied fields $>0.1\ kV\ mm^{-1}$, electro-osmotic fluid flow is observed within the capillaries, as a result of the interaction of the field with the ionic double-layer charge near the capillary wall[19]. In our case, surface charge on the capillary walls arises from adsorption of the positively charged CTAC surfactant[20]. Maintaining a steady fluid flow through the capillaries during the entire growth process ensures that the reactant concentration within each tiny reaction chamber remains constant with time. This constancy is essential for the process and allows uniform films to be grown.

Figure 2 shows scanning electron microscope (SEM) images of lined and two-dimensional patterns of mesoscopic silica grown on a silica substrate after 5 h of reaction time. A d.c. field of $0.15\ kV\ mm^{-1}$ was applied during the entire reaction process, and fresh reacting fluid was continuously dripped on one side of the mould to replenish the volume removed by the electro-osmotic flow. In each case, the patterns formed replicate the structures of the mould. Within the capillaries, films begin to grow on all exposed surfaces, that is, at both the PDMS mould and the substrate/aqueous-solution interface. As the reaction progresses, the capillaries narrow in the centre and eventually seal completely. The high conductivity of the acidic reaction solution gives rise to significant Joule heating at these applied voltages and accelerates the polymerization rate of the TEOS precursor to silica. The dependence of silica polymerization rates on temperature is a well studied phenomenon[21]. Positioning the electrodes in an excess reservoir of reacting solution outside the microcapillary volume (Fig. 1) allows high fields to be applied across the aqueous solution confined within the capillaries. In such a scheme, rapid electrolysis ($H_2O \rightarrow H_2 + 1/2O_2$) ensues, but bubble formation is confined to the fluid reservoir near each electrode and does not disturb the formation of silica mesostructures within the capillaries. With no applied field, 0.5-μm-thick films are typically grown in a period of 24 h but the lines show depressions or discontinuities due to incomplete filling; with an applied field of $0.1\ kV\ mm^{-1}$, similar

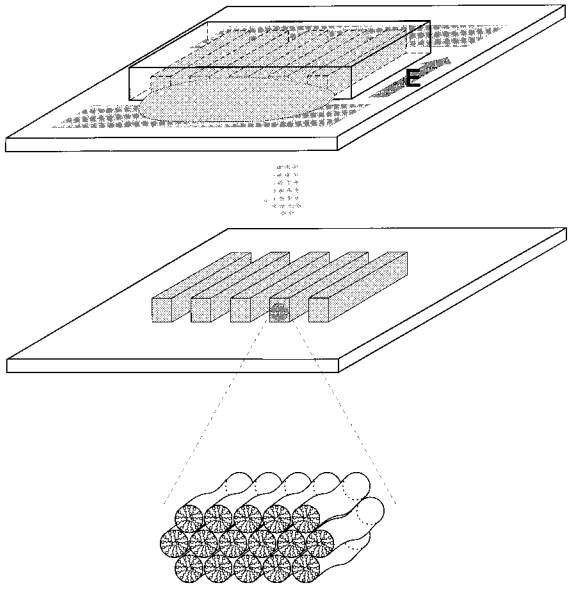

Figure 1 Schematic illustration of the technique used to induce guided growth of mesoscopic silicate structures. The cavity dimensions are not to scale.

‡ Present address: Department of Chemistry, The University of Queensland, St Lucia, Queensland 4072, Australia.

thicknesses are achieved in 1–5 h. Localized heating of the reacting solution in this manner thus provides a useful method of rapidly rigidifying the aligned surfactant tubular structures formed within the microcapillaries.

To determine the orientation of the surfactant nanotubules within these structures, cross-sectional samples were prepared using a Leica ultramicrotome and analysed by transmission electron microscopy (TEM). Figure 3 shows a typical example of the resulting TEM images as well as a typical selected-area electron diffraction (SAED) spot pattern. These reveal a hexagonally packed arrangement of tubules with a nearest-neighbour spacing of 5 nm. Detailed examination of diffraction pattern reveals a slightly distorted packing arrangement, with a deviation of 4% from perfect hexagonal. This distortion may be a result of the accelerated polymerization process described above: with no applied field, no distortion is observed.

Multiple cross-sections were taken of the 1-μm line structures shown in Fig. 2; all these cross-sections appeared identical to the image shown in Fig. 3. This indicates that all tubules within the capillaries are aligned parallel to the substrate, the long axis of the capillary, and the direction of the applied field. The uncalcined samples were very sensitive to the electron beam even at 77 K. Under well-controlled conditions of operation (electron current density at the sample was kept to a low level, $\sim 1\,A\,cm^{-2}$, at 120 keV), the observed hexagonal structure lasts for a few seconds. (The required exposure time is about 2–3 s for the bright-field image and 30–50 s for the SAED pattern.) During this period, most of the regions were unavoidably converted to an amorphous-like structure. After such exposure, the diffused and weak ring-like diffraction pattern observed from a 1-μm^2 area is probably due to the electron beam-induced amorphous-like structure, rather than resulting from a real amorphous structure.

The long-range alignment of the tubules has also been confirmed by X-ray diffraction (XRD) methods (L. Zhou *et al.*, unpublished results). The XRD studies indicated the presence in the uncalcined samples of a minority lamellar phase (<10%) with a lattice spacing of 2.9 nm. The presence of this phase does not alter our claims of the orientation and the continuity of the nanotubules. In the uncalcined samples, orientated and hexagonally packed nanotubules are highly aligned along the surface-normal direction with a mosaic width of <1.7°. This observation strongly suggests that the films are continuous as any discontinuity or twist in the hexagonally packed bundles of nanotubules would have resulted in a much larger mosaic width. The nanotubules are less aligned in the plane parallel to the silicon surface, having a mosaic width of 20°. Preliminary experiments on samples calcined at 400 °C show that the hexagonal phase is retained even after the samples have shrunk by 25%. (Previous work[3,4,22] has shown that surfactants can be removed from mesoporous thin films without degrading the structure significantly.

The long-range alignment is in dramatic contrast to the 'unconfined' mesoscopic silica film synthesis[4], which always results in a disordered, non-aligned arrangement of tubules on amorphous substrates. In our case, rather than taking on a random configuration, growing tubules are guided within the confined space of the capillary and remain parallel to the walls. This orientation occurs either as a result of the action of the external field (that is, alignment of tubules resulting from polarization body forces that operate in regions of dielectric-constant gradient ($\sim \nabla \epsilon E^2$, where ϵ is the local dielectric constant and E is the local electric field; refs 19, 23, 24)) or by virtue of the confined space within which the reaction is performed. In both cases, the tubules would be aligned parallel to the capillary walls. For field-induced alignment, such configurations minimize the overall electrostatic energy—provided that a difference in dielectric constant exists between the inner and outer volume of the tubule. It is also known that the formation of end-caps in self-assembled surfactant cylinders is not favoured, given their high free energy of formation[25]. Thus, within a highly confined region, surfactant cylinders will take on configurations which

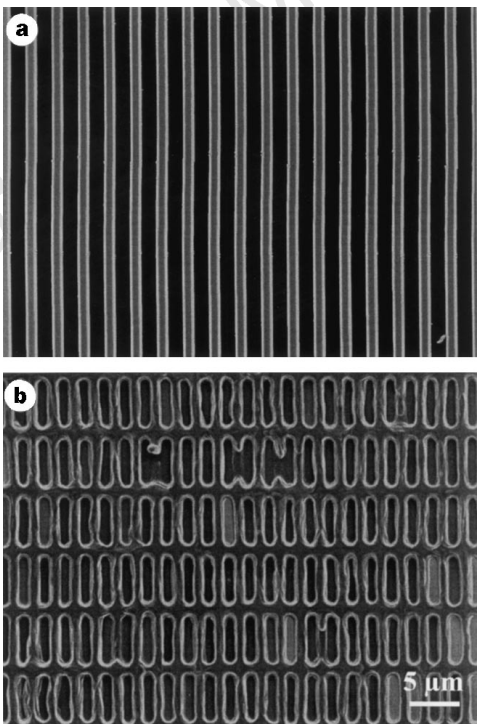

Figure 2 SEM images of 1-μm line (**a**) and two-dimensional (**b**) mesoscopic silicate patterns formed by guided growth within microcapillaries. Electro-osmotic flow is used to transport reacting fluid through the capillaries, and localized Joule heating triggers rapid polymerization of silica around aligned surfactant tubules.

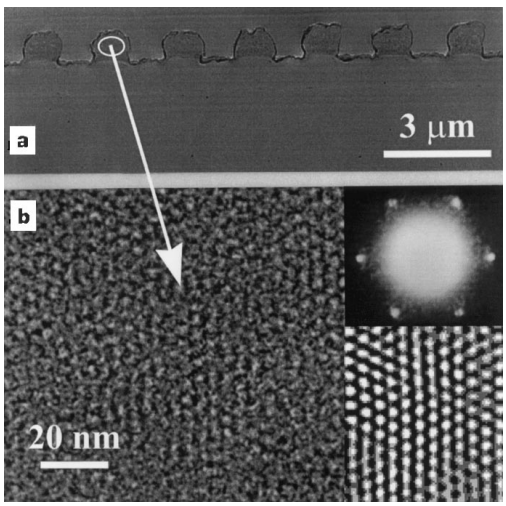

Figure 3 **a** and **b**, TEM images of a patterned mesoscopic silica structure grown on a Thermanox plastic substrate (Electron Microscopy Sciences, Fort Washington, PA). These display a hexagonally packed surfactant tubule structure within the 1-μm-sized lines shown in Fig. 2. The cross-sectional view of each line reveals an identical hexagonally packed pattern of tubules, suggesting global alignment of tubules parallel to the substrate and capillary walls. Similar images have also been obtained for 'confined' films grown on silica substrates. The inset shows (top) the corresponding electron-diffraction pattern obtained from **b**, as well as (bottom) a Fourier transform filtered image. (The same pattern is seen for the full 1 μm^2 region in **a**.) The diffraction pttern reveals a slightly distorted hexagonal lattice with 4% strain. The strain seems to be caused by the rapid polymerization of the inorganic phase induced by localized Joule heating of the confined reacting fluid.

minimize the number of end-caps. Consequently, they will tend to elongate along the long axis of the capillary rather than truncating at capillary walls.

In the absence of an ordering field, a wide range of slowly curving configurations of tubules is routinely observed[4]. In our case, the combined influence of confining geometry and applied field allows the synthesis of silicate nanostructures with precisely controlled geometries. In this way, the tubule geometry is controlled in all regions of the film and the synthesis can be performed on any required substrate, regardless of the nature of the surfactant–substrate interaction. An enormous variety of patterns can be formed using the MIMIC approach, with nanotubules aligned parallel to capillary walls. Capillary thicknesses of 1 μm, corresponding to ~300 nanotubules, are easily achieved by this method and thinner structures can also be formed using moulds formed from masters prepared by electron beam lithography[11].

As a viable method for the production of thin films with complex nanometre- and micrometre-scaled hierarchical architectures, the guided growth of mesoscopic silicates within confined geometries provides a convenient and economic method for fabrication of patterned nanostructured materials. Such materials may be useful in a variety of applications, ranging from sensors and actuators to optoelectronic devices.

Note added in proof: In a recent publication[26], a method has been reported for patterning mesoscopic silica through co-assembly of alkanethiol-decorated gold surfaces. However, nanotubules in these films did not show the orientational order observed in our films. □

Received 18 June; accepted 20 October 1997.

1. Manne, S., Cleveland, J. P., Gaub, G. D., Stucky, G. D. & Hansma, P. K. Direct visualization of surfactant hemimicelles by force microscopy of the electric double layer. *Langmuir* **10,** 4409–4413 (1994).
2. Manne, S. & Gaub, H. E. Molecular organization of surfactants at solid-liquid interfaces. *Science* **270,** 1480–1482 (1995).
3. Yang, H., Kuperman, A., Coombs, N., Mamiche-Afara, S. & Ozin, G. A. Synthesis of oriented films of mesoporous silica on mica. *Nature* **379,** 703–705 (1996).
4. Aksay, I. A. *et al*. Biomimetic pathways for assembling inorganic thin films. *Science* **273,** 892–898 (1996).
5. Kresge, C. T., Leonowicz, M. E., Roth, W. J. & Beck, J. S. Ordered mesoporous molecular sieves synthesized by a liquid-crystal template mechanism. *Nature* **359,** 710–712 (1992).
6. Li, W. Z. *et al*. Large-scale synthesis of aligned carbon nanotubes. *Science* **274,** 1701–1703 (1996).
7. Sakai, H., Baba, R., Hashimoto, K., Fujishima, A. & Heller, A. Local detection of photoelectrochemically produced H_2O_2 with a "wired" horseradish peroxidase microsensor. *J. Phys. Chem.* **99,** 11896–11900 (1996).
8. Linder, E. *et al*. Flexible (kapton-based) microsensor arrays of high stability for cardiovascular applications. *J. Chem. Soc. Faraday Trans.* **89,** 361–367 (1993).
9. Tamagawa, C. Y., Schiller, P. & Polla, D. L. Pyroelectric $PbTiO_3$ thin films for microsensensor applications. *Sensors Actuators A* **35,** 77–83 (1992).
10. Fendler, J. H. Self assembled nanostructured materials. *Chem. Mater.* **8,** 1616–1624 (1996).
11. Kim, E., Xia, Y. & Whitesides, G. M. Polymer microstructures formed by moulding in capillaries. *Nature* **376,** 581–584 (1995).
12. Broers, A. N., Harper, J. M. & Molzen, W. W. 250-Å linewidths with PMMA electron resist. *Appl. Phys. Lett.* **33,** 392–394 (1978).
13. Fischer, P. B. & Chou, S. Y. 10 nm electron beam lithography and sub-50 nm overlay using a modified scanning electron microscope. *Appl. Phys. Lett.* **62,** 2989–2991 (1993).
14. Flanders, D. Replication of 175-Å lines and spaces in polymethylmethacrylate using x-ray lithography. *Appl. Phys. Lett.* **36,** 93–96 (1980).
15. Early, K., Schattenberg, M. L. & Smith, H. I. Absence of resolution degradation in x-ray lithography for λ from 4.5 nm to 0.83 nm. *Microelectron. Eng.* **11,** 317–321 (1990).
16. McCord, M. A. & Pease, R. F. P. Lithography with the scanning tunneling microscope. *J. Vac. Sci. Technol. B* **4,** 86–87 (1986).
17. Kramer, N., Birk, J., Jorvitsma, M. & Schronenberger, C. Fabrication of metallic nanowires with a scanning tunneling microscope. *Appl. Phys. Lett.* **66,** 1325–1327 (1995).
18. Chou, S. Y., Krauss, P. R. & Renstrom, P. J. Imprint lithography with 25-nanometer resolution. *Science* **272,** 85–87 (1996).
19. Russel, W. B., Saville, D. A. & Schowalter, W. R. *Colloidal Dispersions* 212–235 (Cambridge Univ. Press, New York, 1989).
20. Scales, P. J., Grieser, F., Healy, T. W. & Magid, L. J. Electrokinetics of muscovite mica in the presence of adsorbed cationic surfactants. *Langmuir* **8,** 277–282 (1992).
21. Iler, R. K. *The Colloid Chemistry of Silica and Silicates* 36–69 (Cornell Univ. Press, Ithaca, 1955).
22. Lu, Y. *et al*. Continuous formation of supported cubic and hexagonal mesoporous films by sol-gel dip-coating. *Nature* **389,** 364–368 (1997).
23. Morkved, T. L. *et al*. Local control of microdomain orientation in diblock copolymer thin films with electric fields. *Science* **273,** 931–933 (1996).
24. Amundson, K. *et al*. Effect of an electric field on block copolymer microstructure. *Macromolecules* **24,** 6546–6548 (1991).
25. Israelachvili, J. *Intermolecular and Surface Forces* 374 (Academic, London, 1992).
26. Yang, H., Coombs, N. & Ozin, G. A. Mesoporous silica with micrometer-scale designs. *Adv. Mater.* **9,** 811–814 (1997).

Acknowledgements. We thank L. Zhou, P. Fenter and P. M. Eisenberger for the X-ray diffraction characterization of the films. This work was supported by a MURI grant from the US Army Research Office and made use of the central facilities supported by an MRSEC programme of the NSF.

Correspondence and requests for materials should be addressed to I.A.A. (e-mail: iaksay@princeton.edu).

A resonance in the Earth's obliquity and precession over the past 20 Myr driven by mantle convection

Alessandro M. Forte* & Jerry X. Mitrovica†

* *Institut de Physique du Globe de Paris, Département de Sismologie, 4 place Jussieu, Tour 24-étage 4, 75252 Paris Cedex 05, France*
† *Department of Physics, University of Toronto, 60 St George Street, Toronto, M5S 1A7, Canada*

The motion of the Solar System is chaotic to the extent that the precise positions of the planets are predictable for a period of only about 20 Myr (ref. 1). The Earth's precession, obliquity and insolation parameters over this time period[1–6] can be influenced by secular variations in the dynamic ellipticity of the planet which are driven by long-term geophysical processes, such as post-glacial rebound[5,7–10]. Here we investigate the influence of mantle convection on these parameters. We use viscous flow theory to compute time series of the Earth's dynamic ellipticity for the past 20 Myr and then apply these perturbations to the nominal many-body orbital solution of Laskar *et al.*[5]. We find that the convection-induced change in the Earth's flattening perturbs the main frequency of the Earth's precession into the resonance associated with a secular term in the orbits of Jupiter and Saturn[5], and thus significantly influences the Earth's obliquity. We also conclude that updated time series of high-latitude summer solar insolation diverge from the nominal solution for periods greater than the past ~5 Myr. Our results have implications both for obtaining precise solutions for precession and obliquity and for procedures that adopt astronomical calibrations to date sedimentary cycles and climatic proxy records.

In many-body orbital calculations, the Earth has traditionally been treated as a non-deformable body[1,2] with the possible exception of changes in shape associated with tidal dissipation[4]. Recently, some studies have adopted viscoelastic models to investigate perturbations in the Earth's dynamic ellipticity due to surface mass load variations associated with the late Pleistocene ice-age cycles[8,9]. These studies were motivated by Laskar *et al.*[5], who suggested that the effect of the ice ages might be sufficient to perturb the Earth's precession and obliquity into a resonance due to the $s_6 - g_6 + g_5$ forcing associated with orbital elements of Jupiter and Saturn. Although this is now believed to be unlikely[8,9], the ice-age effect will nevertheless influence astronomical calibrations of Quaternary geological core-records[10]. Over periods comparable to the span of current orbital integrations (~20 Myr), secular variations in the dynamic ellipticity of the Earth may arise from a number of geophysical processes, but will be dominated by convective flow in a viscous mantle. The influence of this process on the precession and obliquity of the Earth has not been previously considered.

The dynamic ellipticity of the Earth is defined as

$$H(t) = \frac{C(t) - \frac{1}{2}[A(t) + B(t)]}{C(t)} \qquad (1)$$

where C is the polar moment of inertia, A and B are the principal equatorial moments of inertia and t is the time. In the case of a compressible, self-gravitating, newtonian viscous mantle, perturbations in the ellipticity can be computed using the equation[11]

$$\delta H(t) = -\frac{4\pi a^4}{\sqrt{5}C}\int_{r_{cmb}}^{a} G_2\left[\nu(r)\Big/\nu_o; r\right]\delta\rho_2^0(r,t)\mathrm{d}r \qquad (2)$$